ER-stress mobilization of death-associated protein kinase-1–dependent xenophagy counteracts mitochondria stress–induced epithelial barrier dysfunction

Received for publication, November 6, 2017, and in revised form, December 21, 2017 Published, Papers in Press, January 9, 2018, DOI 10.1074/jbc.RA117.000809

Fernando Lopes[‡1], Åsa V. Keita[§], Alpana Saxena[‡], Jose Luis Reyes[‡], Nicole L. Mancini[‡], Ala Al Rajabi[‡], Arthur Wang[‡], Cristiane H. Baggio[‡], Michael Dicay[‡], Rob van Dalen[¶], Younghee Ahn[‖], Matheus B. H. Carneiro[**], Nathan C. Peters[**], Jong M. Rho[‖], Wallace K. MacNaughton[‡], Stephen E. Girardin[¶], Humberto Jijon[‡‡], Dana J. Philpott[§§], Johan D. Söderholm[§], and Derek M. McKay[‡2]

*From the Gastrointestinal Research Group, Departments of [‡]Physiology and Pharmacology and [‡‡]Medicine, Calvin, Joan, and Phoebe Snyder Institute for Chronic Diseases, and the [‖]Departments of Pediatrics, Clinical Neurosciences, and Physiology and Pharmacology and the **Department of Microbiology, Immunology and Infectious Diseases, Cumming School of Medicine, University of Calgary, Calgary, Alberta T2N4N1, Canada, the [§]Department of Clinical and Experimental Medicine, Division of Surgery, Linköping University, Linköping 581 83, Sweden, and the Departments of [¶]Laboratory Medicine and Pathobiology and [§§]Immunology, University of Toronto, Toronto, Ontario M5S1A1, Canada*

Edited by Ursula Jakob

The gut microbiome contributes to inflammatory bowel disease (IBD), in which bacteria can be present within the epithelium. Epithelial barrier function is decreased in IBD, and dysfunctional epithelial mitochondria and endoplasmic reticulum (ER) stress have been individually associated with IBD. We therefore hypothesized that the combination of ER and mitochondrial stresses significantly disrupt epithelial barrier function. Here, we treated human colonic biopsies, epithelial colonoids, and epithelial cells with an uncoupler of oxidative phosphorylation, dinitrophenol (DNP), with or without the ER stressor tunicamycin and assessed epithelial barrier function by monitoring internalization and translocation of commensal bacteria. We also examined barrier function and colitis in mice exposed to dextran sodium sulfate (DSS) or DNP and co-treated with DAPK6, an inhibitor of death-associated protein kinase 1 (DAPK1). Contrary to our hypothesis, induction of ER stress (*i.e.* the unfolded protein response) protected against decreased barrier function caused by the disruption of mitochondrial function. ER stress did not prevent DNP-driven uptake of bacteria; rather, specific mobilization of the ATF6 arm of ER stress and recruitment of DAPK1 resulted in enhanced autophagic killing (xenophagy) of bacteria. Of note, epithelia with a Crohn's disease–susceptibility mutation in the autophagy gene *ATG16L1* exhibited less xenophagy. Systemic delivery of the DAPK1 inhibitor DAPK6 increased bacterial translocation in DSS- or DNP-treated mice. We conclude that promoting ER stress–ATF6–DAPK1 signaling in transporting enterocytes counters the transcellular passage of bacteria evoked by dysfunctional mitochondria, thereby reducing the potential for metabolic stress to reactivate or perpetuate inflammation.

Bacteria within the epithelium are a pro-inflammatory threat. While observed in inflammatory bowel disease (IBD)[3] (1–4), and putatively important in disease pathophysiology, the mechanism(s) underlying this barrier defect is unclear. Mutation in the organic cation transporter (*OCTN2*) gene is a susceptibility trait for IBD (5); this transporter facilitates carnitine uptake for fatty acid β-oxidation and ATP generation. Moreover, deranged mitochondrial ultrastructure, loss of mitochondrial proteins, lower levels of ATP, and increased susceptibility to uncouplers of oxidative phosphorylation occur in some patients with IBD (6). Similarly, suspected triggers of IBD reactivation can perturb mitochondrial function. For instance, nonsteroidal anti-inflammatory drugs (NSAID) can cause relapses in IBD (7), and their use damages mitochondria contributing to decreased enteric barrier function (8, 9). Consequently, mitochondria are emerging as an organelle of interest in IBD and other enteropathies (10).

While idiopathic, the consensus is that uncontrolled immune reactivity against a component(s) of the gut microbiota in a genetically susceptible individual causes IBD (11). A defect in epithelial barrier function is implied in this hypothesis. With the exceptions of uptake by microfold cells or dendritic

This work was supported in part by Canadian Institutes for Health Research Operating Grant MPO-126005 (to D. M. M.). The authors declare that they have no conflicts of interest with the contents of this article.

This article contains Figs. S1–S5.

[1] Supported by Canadian Institutes for Health Research/Canadian Association of Gastroenterology/Allergan, Inc., and Alberta Innovates-Health Solutions post-doctoral fellowships. To whom correspondence may be addressed: Dept. of Physiology and Pharmacology, University of Calgary, Hsc 1877, 3330 Hospital Dr. NW, Calgary, Alberta T2N4N1, Canada. Tel.: 403-220-7362; E-mail: flopes77@gmail.com.

[2] Holds a Canada Research Chair (CRC, Tier 1) in Intestinal Immunophysiology in Health and Disease. To whom correspondence may be addressed: Dept. of Physiology and Pharmacology, University of Calgary, Hsc 1877, 3330 Hospital Dr. NW, Calgary, Alberta T2N4N1, Canada. Tel.: 403-220-7362; E-mail: dmckay@ucalgary.ca.

[3] The abbreviations used are: IBD, inflammatory bowel disease; DNP, dinitrophenol; ER, endoplasmic reticulum; DSS, dextran sodium sulfate; NSAID, non-steroidal anti-inflammatory drug; MLN, mesenteric lymph node; cfu, colony-forming unit; TUNEL, terminal deoxynucleotidyltransferase-mediated dUTP nick-end labeling; TER, transepithelial resistance; ROS, reactive oxygen species; UPR, unfolded protein response; PERK, pancreatic ER kinase; TM, tunicamycin; 3-MA, 3-methyladenine; JNK, c-Jun N-terminal kinase; DAPI, 4′,6-diamidino-2-phenylindole.

cell pseudopodia, material in the gut lumen enters the submucosa via the epithelial tight junctions (paracellular) or by crossing the enterocyte (transcellular) (12), and regulation of both pathways is energy-dependent. With that, it can be proposed that perturbed epithelial mitochondrial function would increase gut permeability to initiate disease or to precipitate relapses in IBD. Accordingly, mitochondrial damage induced by uncoupling oxidative phosphorylation with the H^+ ionophore, dinitrophenol (DNP), to model the mitochondrial dysfunction observed in IBD resulted in increased internalization into and transcytosis of *Escherichia coli* across epithelial monolayers (13–15).

Mitochondria couple with the endoplasmic reticulum (ER), where reactive oxygen species (ROS) are important in protein folding (16). When improperly folded proteins accumulate in the ER, an ER stress program (or unfolded protein response (UPR)) occurs. Mice deficient in any of the three major arms of the ER stress response (inositol-requiring kinase/endonuclease 1 (IRE1), pancreatic ER kinase (PERK), and activating transcription factor 6 (ATF6)) are more susceptible to DSS-induced colitis (17, 18). Furthermore, mutation in the X-box–binding protein-1 (*XBP1*) gene (downstream of IRE1) is a susceptibility trait for Crohn's disease (17), and increased ER stress can occur in the epithelium of patients with IBD (17, 19, 20). We hypothesized that uncoupling oxidative phosphorylation (*i.e.* mitochondrial dysfunction) combined with ER stress would severely compromise epithelial integrity.

Results

ER stress protects epithelium transcellular permeability perturbed by mitochondrial stress

Human colonic biopsies were mounted in Ussing chambers; bacteria were added to the luminal buffer, and biopsies were treated with DNP ± the ER stressor tunicamycin (blocks protein glycosylation (21), which is often used to elicit ER stress in cell lines (19)). DNP promoted *E. coli* uptake; however, tunicamycin reduced this barrier defect (Fig. 1*A*). DNP treatment of colonic enteroid monolayers resulted in increased transcytosis of *E. coli* that was reduced by tunicamycin (Fig. 1*B*). Similarly, DNP-evoked increases in bacterial internalization into and translocation across the T84 (Fig. 1, *C* and *D*), Caco-2 (Fig. S1*A*), and HCT116 (Fig. S1*B*) human epithelial cell lines was significantly reduced by tunicamycin co-treatment. (Tunicamycin induction of ER stress was confirmed by GRP78 expression (Fig. S1*C*). Tunicamycin did not increase intracellular *E. coli* (Fig. S1*D*).) The NSAID indomethacin increased intracellularly viable *E. coli* in T84 cells (9), and this was reduced by tunicamycin (Fig. 1*E*). (HeLa cells provided similar data (Fig. S2).) Treatment with other ER stressors, brefeldin A (blocks Golgi transit) or thapsigargin (Ca^{2+}-ATPase blocker that perturbs ER Ca^{2+} stores) (22), also reduced the number of viable intracellular bacteria after exposure to DNP (Fig. 1*F*). Epithelia treated with DNP display decreased TER (Fig. 1*G*) and increased FITC-dextran flux (Fig. 1*H*), and tunicamycin did not affect the increased paracellular permeability (Fig. 1, *G* and *H*). Respiratory rate (basal respiration, maximal respiration, and respiratory capacity) and ATP synthesis were reduced by DNP, and these bioenergetic parameters were not restored in tunicamycin co-treated cells (Fig. S3, *A–C*) (glycolysis was unaffected by DNP ± tunicamycin (Fig. S3*D*)).

Analysis of the 16 h post-DNP + *E. coli* ± tunicamycin exposure revealed no significant increase in T84 cell apoptosis; however, there was an ~50% decrease in viability by 36 h post-DNP + *E. coli* treatment that was significantly reduced by tunicamycin (Fig. S4).

Tunicamycin promotes killing of internalized bacteria

Reduced numbers of intracellular bacteria could reflect a reduction in extracellular bacteria; analysis at the end of each experiment revealed no significant differences in the extracellular bacteria numbers between the groups. The reduced number of viable intracellular *E. coli* in DNP + tunicamycin co-treated epithelia could be due to uptake inhibition. Immunolocalization (Fig. 2*A*) and flow cytometry (Fig. 2*B*) revealed tunicamycin did not affect the DNP-induced internalization of inert fluorescent beads, suggesting that inhibition of the rate of *E. coli* internalization is not the cause of the reduced viable bacteria in DNP + tunicamycin-treated T84 epithelia. However, the DNP-induced increase in inert *E. coli* (K-12) fluorescent bioparticles was abrogated by co-treatment with tunicamycin (Fig. 2*C*), suggestive of degradation and loss of fluorescence.

E. coli + DNP + tunicamycin-treated epithelia displayed enhanced autophagy as gauged by increased expression of LC3-II and beclin-1 and LC3 immunostaining (Fig. 2, *D* and *E*). Postulating that autophagy would target the internalized bacteria (*i.e.* xenophagy), co-localization of autophagosomes and internalized bacteria was observed in DNP + tunicamycin-treated cells (Fig. 2*E*). Furthermore, tunicamycin antagonism of DNP-induced *E. coli* internalization was lost in cells lacking the autophagy protein ATG16L1 (Fig. 3, *A* and *B*). Also, tunicamycin inhibition of the DNP-induced increased viable intracellular *E. coli* was not apparent in colonoids from mice expressing the knocked-in variant of $Atg16l1^{T316A}$ (homologous to the IBD susceptibility trait $ATG16L1^{T300A}$) (Fig. 3, *C* and *D*). These findings suggest that ER stress ablated the DNP effect by mobilizing autophagy to kill the bacteria. In accordance, rapamycin (induces autophagy (23)) significantly reduced the number of viable intracellular bacteria and translocation across T84 cell monolayers (Fig. 4, *A* and *B*). Autophagy inhibition with 3-MA increased numbers of viable bacteria in tunicamycin-treated wildtype T84 cells (Fig. 4*C*). Moreover, rapamycin prevented the DNP-induced increase in live *E. coli* HS transcytosis across human colonic biopsies (Fig. 4*D*). Like tunicamycin, rapamycin did not affect the DNP-induced drop in TER or FITC-dextran flux across T84 epithelia (Fig. 4, *E* and *F*). Although the ability of tunicamycin to induce xenophagy was lost in ATG16L1 transgenic cells, tunicamycin reduced the number of viable bacteria in DNP-treated $NOD2^{-/-}$ T84 cells (Fig. 4*G*).

These data are in accordance with the supposition by Adolph *et al.* (24) that the ER stress observed in patients with IBD could compensate for defective/reduced autophagy, and, we add, a reaction to increased transcellular transport of commensal bacteria.

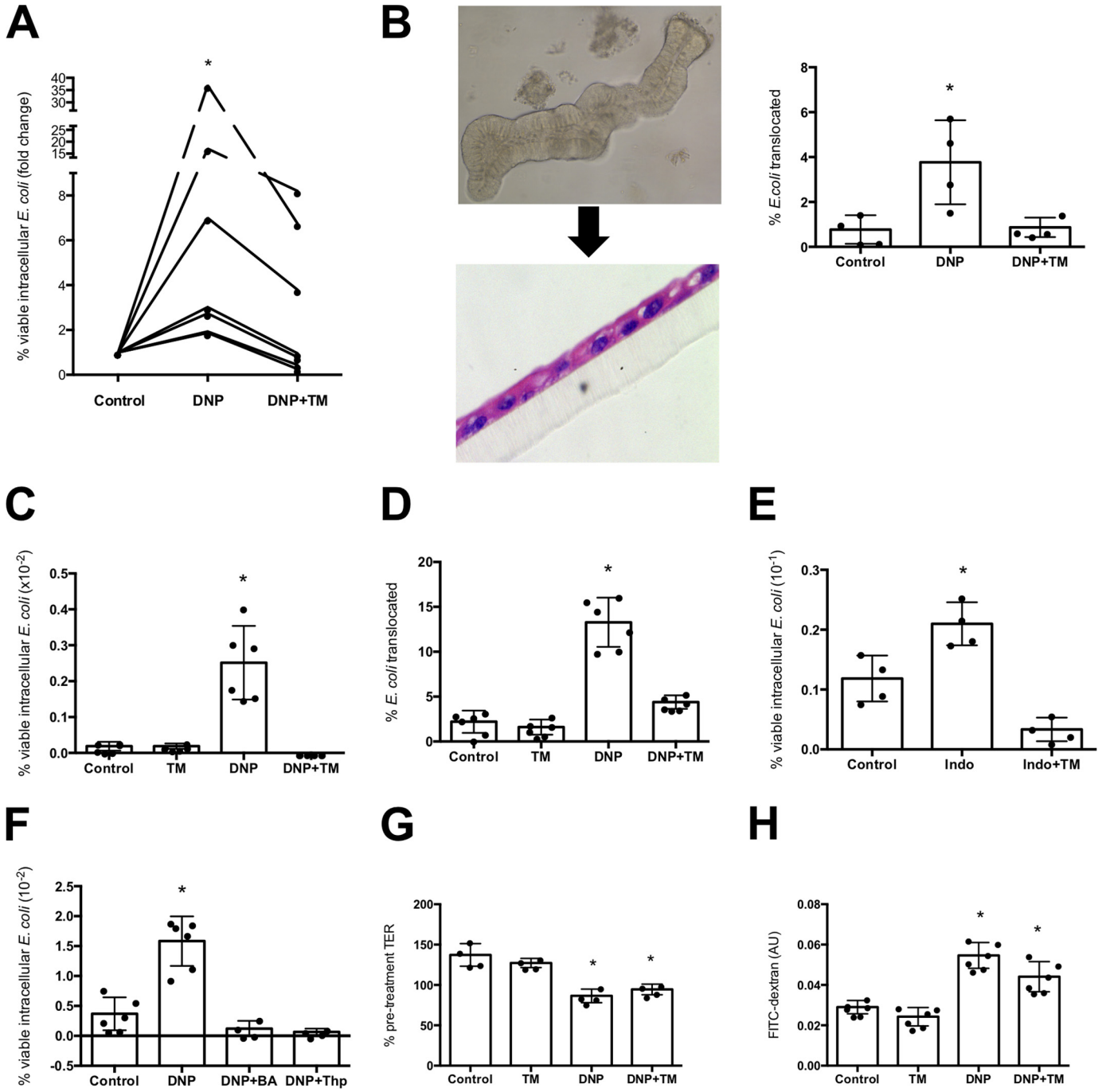

Figure 1. ER stress protects against epithelial barrier dysfunction evoked by metabolic stress. *A,* human colonic biopsies were mounted in Ussing chambers, live green fluorescent protein-labeled *E. coli* HS (10^8 cfu/ml) ± the metabolic stressor DNP (0.1 mM) or the ER stressor tunicamycin (*TM*, 10 μg/ml) added to the luminal side, and translocation into the serosal buffer assessed 3 h later ($n = 7$; *, $p < 0.05$ compared with control). *B,* mouse colonic enteroids were grown for 7 days, resuspended, and grown as monolayer, and then *E. coli* (strain HB101, 10^7 cfu) was added to the luminal surface ± DNP (0.1 mM) ± TM (10 μg/ml), and bacterial translocation into the basal compartment of the culture well was determined 16 h later (*insets,* phase contrast images of enteroid and subsequent filter-grown monolayer (10-μm section stained with hematoxylin and eosin)). *C,* monolayers of the human colon-derived T84 cells were grown to confluence (*i.e.* starting TER = 1000–1800 ohms·cm^2) or to ~70% confluence (by phase microscopy) on 12-well plates. Epithelia were treated with *E. coli* (strain HB101, 10^6 cfu) and DNP ± TM. Bacterial translocation from the apical surface of the epithelium into the basal compartment of the culture well (*D*) and bacterial internalization (as % of extracellular *E. coli*) were assessed 16 h later (one representative experiment of six experiments). *E,* increased epithelial (T84 cells) internalization of *E. coli* induced by the NSAID, indomethacin (*indo*; 1 μM; 16 h treatment), was reduced by TM co-treatment ($n = 4$ epithelial monolayers). *F*, shows the effect of two other ER stressors brefeldin-A (*BA*, 1 μM) and thapsigargin (*Thp,* 2 μM) on DNP-induced (16 h) T84 cell internalization of *E. coli* ($n = 4–6$). *G* and *H* show markers of paracellular permeability, TER, at 16 h post-treatment (normalized and presented as % pre-treatment value), and flux of 4-kDa FITC-dextran (100 μg/ml) over a 4-h period (after 16-h treatments) (1 representative experiment of two experiments) (mean ± S.D.; *, $p < 0.05$ compared with control).

ATF-6 mediates inhibition of the DNP-effect

ER stress triggers three major pathways: IRE1 that activates the mitogen-activated protein kinase, JNK, and splicing of XBP1 transcription factor; PERK that leads to eIF2α phosphorylation, which acts as a transcription factor, and ATF4 mobilization, another transcription factor; and ATF6 that when

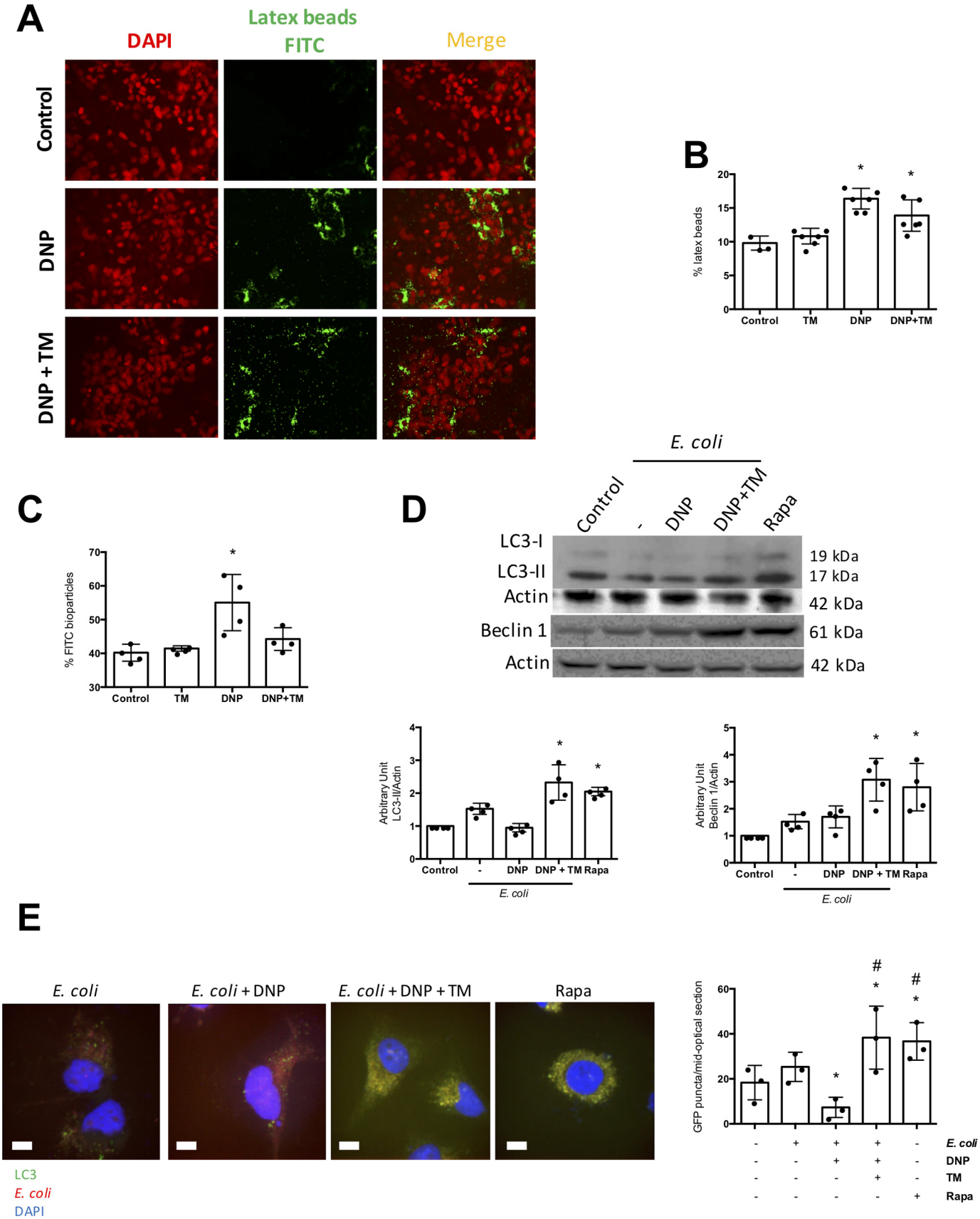
A
DAPI
Latex beads
FITC
Merge
Control
DNP
DNP + TM
B
% latex beads
Control
TM
DNP
DNP+TM
C
% FITC bioparticles
Control
TM
DNP
DNP+TM
D
E. coli
Control
-
DNP
DNP+TM
Rapa
LC3-I
LC3-II
Actin
Beclin 1
Actin
19 kDa
17 kDa
42 kDa
61 kDa
42 kDa
Arbitrary Unit
LC3-II/Actin
Control
-
DNP
DNP + TM
Rapa
E. coli
Arbitrary Unit
Beclin 1/Actin
Control
-
DNP
DNP + TM
Rapa
E. coli
E
E. coli
E. coli + DNP
E. coli + DNP + TM
Rapa
LC3
E. coli
DAPI
GFP puncta/mid-optical section
E. coli
DNP
TM
Rapa

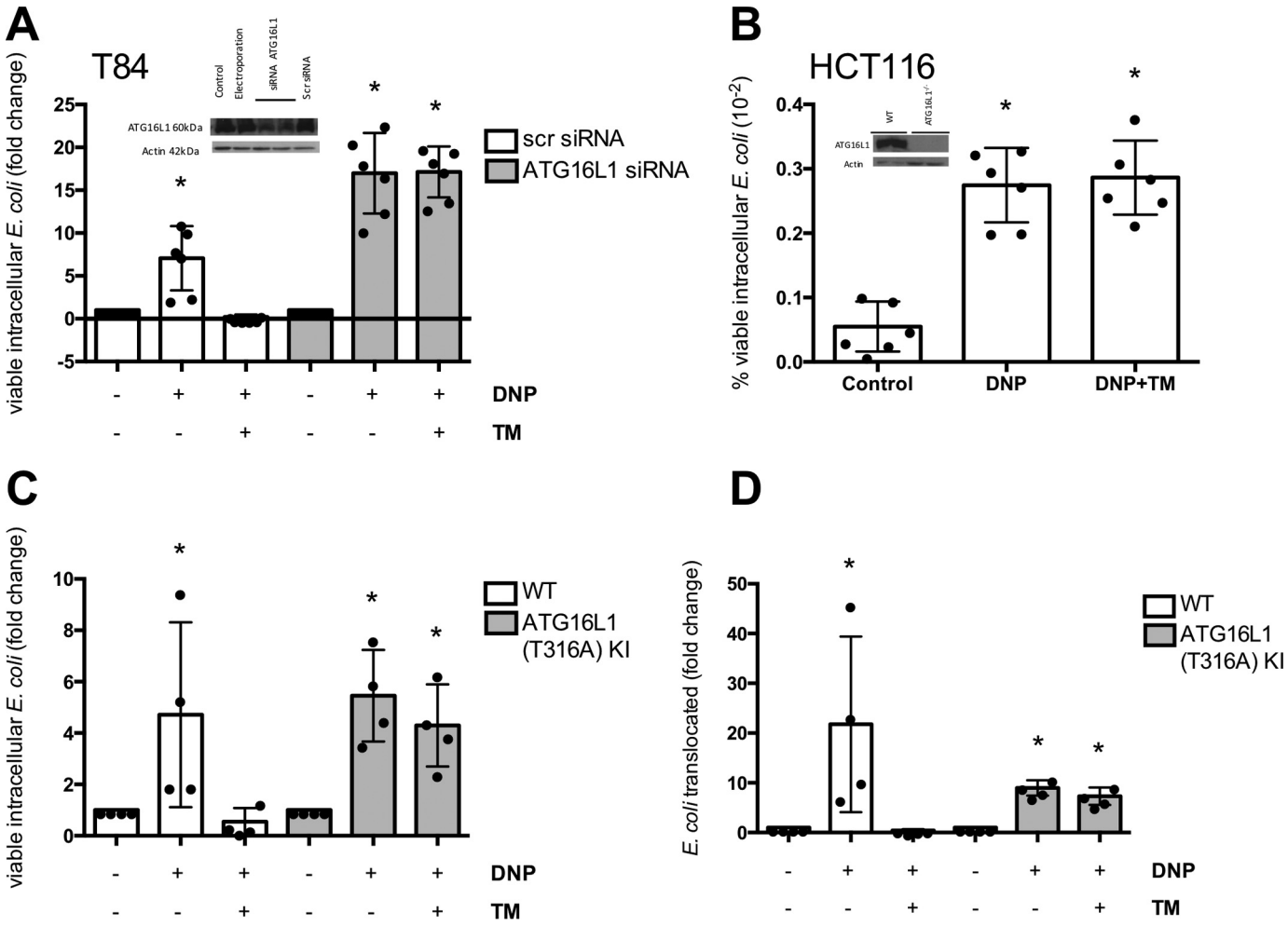

Figure 3. Role of autophagy in ER stress protection of metabolic stress–induced barrier defect. The autophagy *ATG16L1* gene was knocked down by siRNA (T84 cells) (*A*) or knocked out with CRISPR-Cas9 (HCT116 cells) (*B*). The cells were exposed to *E. coli* (10^6 cfu, strain HB101) and DNP (0.1 mM) ± TM (10 μg/ml) for 16 h, and the number of viable intracellular bacteria was assessed (one representative experiment of two experiments). Internalization (*C*) and translocation (*D*) of *E. coli* HB101 (10^7, cfu) across colonoids from mice with the knockin (*KI*) of $ATG16L1^{T316A}$ grown as monolayers on filter supports and treated with DNP ± TM for 16 h (mean ± S.D.; *, $p < 0.05$ compared with control).

truncated serves as a transcription factor (25). Tunicamycin resulted in subtle but significant increase in spliced XBP1, ATF4, and ATF6α in T84 cells (Fig. 5*A*). Transient siRNA knockdown of ATF6α, PERK, or IRE1 in T84 cells revealed that only the former blocked tunicamycin inhibition of DNP-evoked increases in viable intracellular *E. coli* (Fig. 5*B*). Selective pharmacological inhibitors of JNK (p-JNK increased in the cells) (Fig. 5*C*), IRE1, and PERK did not affect tunicamycin abrogation of the DNP effect (Fig. 5, *D* and *E*), focusing attention on ATF6. The increase in autophagy (*i.e.* LC3-II protein expression) evoked by tunicamycin was absent in ATF6α siRNA-treated T84 cells (Fig. 5*F*).

DAP kinase-1 is needed for tunicamycin inhibition of DNP-evoked decreased barrier function

DAPK1 is mobilized downstream of ATF6 to regulate autophagy and apoptosis (26). T84 epithelia exposed to *E. coli* + DNP + tunicamycin displayed increased DAPK1 expression compared with cells treated with ATF6 siRNA (Fig. 6*A*) (PERK and IRE1 siRNA did not inhibit DAPK1 protein expression (Fig. S5)). Use of a selective DAPK1 inhibitor, designated DAPK6, blocked tunicamycin's ability to reduce DNP-evoked increases in viable intracellular *E. coli* by T84 cells (Fig. 6*B*) and the mobilization of autophagy (Fig. 6, *C* and *D*). Moreover,

Figure 2. Tunicamycin promotes killing of internalized bacteria and not suppression of uptake. T84 epithelial cells were incubated with fluorescent latex beads (10^8 1-μm diameter), DNP (0.1 mM), or DNP + TM (10 μg/ml) for 16 h, and monolayers were assessed by fluorescence microscopy (representative images, ×40 magnification) (*A*) and (*B*) flow cytometry (*B*). *C,* in parallel cultures, flow cytometry was used to assess intracellular levels of fluorescent dead *E. coli* F12 bioparticles (10^6/ml). *D,* T84 cells were treated with *E. coli* (HB101, 10^6 cfu) ± DNP or DNP + TM for 16 h, and autophagy was assessed by expression of LC3-II and beclin-1 on immunoblots that were quantified by densitometry and normalized to actin expression. Rapamycin (*Rapa*; 100 nM, 16 h) was a positive control for the induction of autophagy. *E,* LC3-GFP HeLa cells were treated as shown for 16 h and GFP^+ puncta counted in randomly selected cells based on DAPI nuclear staining (representative images; *scale bar,* 65 μm). Co-localization of bacteria in phagosomes was obvious in the *E. coli* + DNP + TM-treated cells (mean ± S.D.; * and #, $p < 0.05$ compared with control and *E. coli*+ DNP-treated cells, respectively).

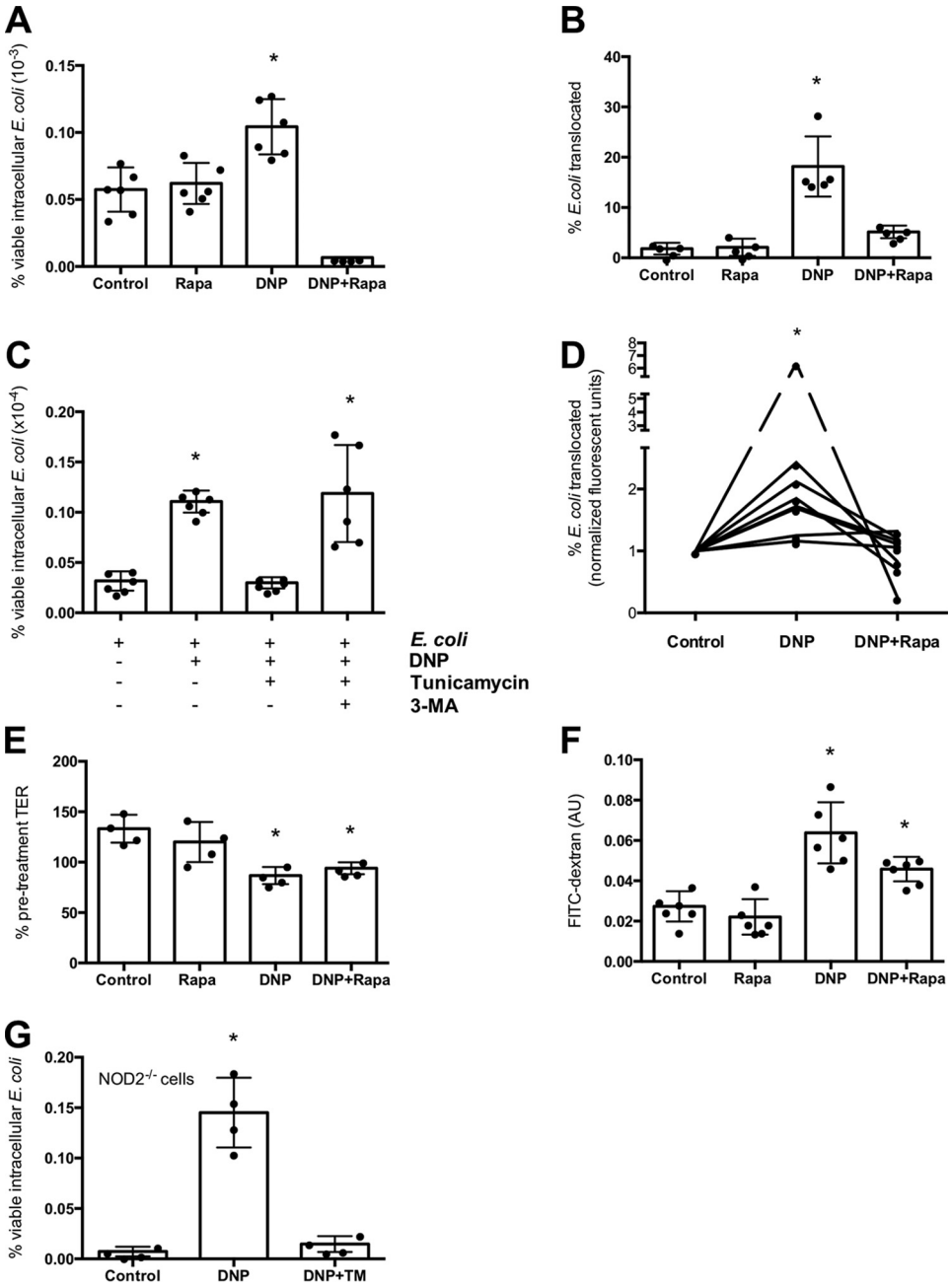

Figure 4. Induction of autophagy prevents DNP-induced barrier defect. The inducer of autophagy, rapamycin (*Rapa*, 100 nM, 16 h), blocked the effect of DNP on T84 epithelial cell internalization (*A*) and translocation (*B*) of bacteria across filter-grown monolayers. *C*, T84 cell treated with *E. coli* (strain HB101; 10^6 cfu) and DNP (0.1 mM) ± TM (10 μg/ml) ± the autophagy inhibitor 3-MA (5 μM) and bacterial internalization assessed 16 h later. *D*, increased mucosal-to-serosal flux of live green fluorescent protein-labeled *E. coli* HS across Ussing-chambered human colonic biopsies (*DNP* ± *Rapa* for 3 h). Rapamycin did not affect the DNP-induced reduction in TER (*E*) or the concomitant increased flux of 4-kDa FITC-dextran across T84 cell monolayers (*F*) (one representative experiment of two experiment s). *G*, T84 cells in which *NOD2* was knocked out using shRNA also display increased DNP-induced internalization of *E. coli* that is inhibited by TM co-treatment (mean ± S.D.; *, $p < 0.05$ compared with control).

bacteria–autophagosome co-localization was completely lost in DAPK6 co-treated cells (Fig. 6*D*).

Likewise, knockdown of DAPK1 in T84 cells resulted in inhibition of the tunicamycin effect and increased viable intracellular *E. coli* numbers (Fig. 7*A*). Although the activation of ATF6 was not affected by DAPK1 siRNA in DNP + *E. coli* + tunicamycin-treated epithelia, the increased autophagy was lost, showing that the signal needed to up-regulate autophagy by ER stress was interrupted in the absence of DAPK1 (Fig. 7*B*). Co-treatment with DAPK1 siRNA and DAPK6 prevented the ability of tunicamycin to block the effects of DNP, but to a degree that was not statistically different from either DAPK6 or DAPK1 siRNA alone (Fig. 7*C*). These data also support the specificity of DAPK6 in targeting DAPK1, an important observation in the context of the murine *in vivo* experiments presented below.

Mice treated with DAPK6 were more susceptible to DSS-induced colitis as gauged by disease activity score (Fig. 8*A*), colon length (Fig. 8*B*), and weight loss (Fig. 8*C*). DAPK6 treatment resulted in increased translocation of aerobic bacteria

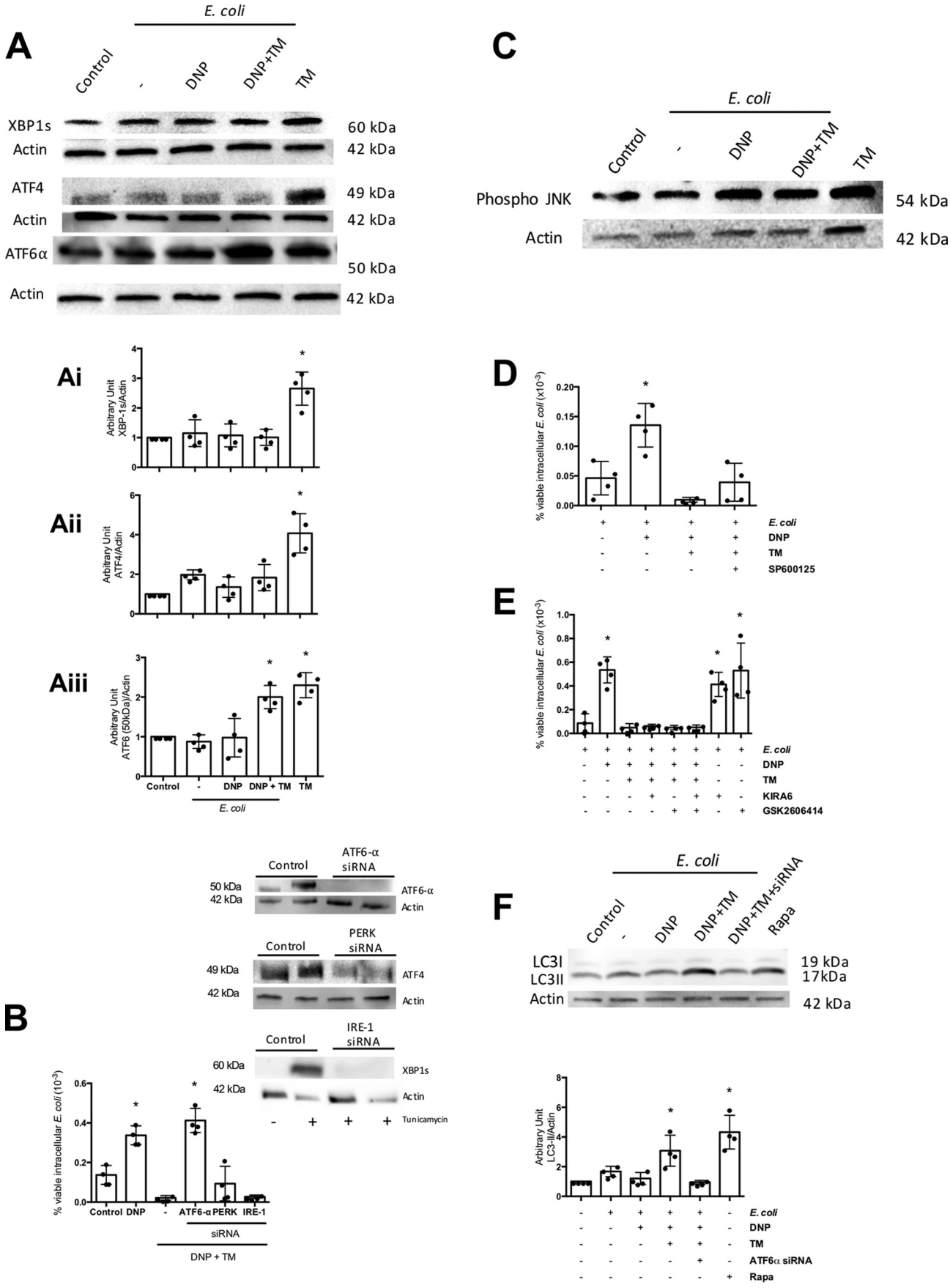
A
E. coli
Control
-
DNP
DNP+TM
TM
XBP1s
60 kDa
Actin
42 kDa
ATF4
49 kDa
Actin
42 kDa
ATF6α
50 kDa
Actin
42 kDa
Ai
Arbitrary Unit XBP-1s/Actin
Aii
Arbitrary Unit ATF4/Actin
Aiii
Arbitrary Unit ATF6 (50kDa)/Actin
Control
-
DNP
DNP + TM
TM
E. coli
B
Control
ATF6-α siRNA
50 kDa
42 kDa
ATF6-α
Actin
Control
PERK siRNA
49 kDa
ATF4
42 kDa
Actin
Control
IRE-1 siRNA
60 kDa
XBP1s
42 kDa
Actin
- + + + Tunicamycin
% viable intracellular E. coli (10-3)
Control DNP - ATF6-α PERK IRE-1
siRNA
DNP + TM
C
E. coli
Control
-
DNP
DNP+TM
TM
Phospho JNK
54 kDa
Actin
42 kDa
D
% viable intracellular E. coli (x10-3)
E. coli
DNP
TM
SP600125
E
% viable intracellular E. coli (x10-3)
E. coli
DNP
TM
KIRA6
GSK2606414
F
E. coli
Control
-
DNP
DNP+TM
DNP+TM+siRNA
Rapa
LC3I
LC3II
19 kDa
17kDa
Actin
42 kDa
Arbitrary Unit LC3-II/Actin
E. coli
DNP
TM
ATF6α siRNA
Rapa

into the colonic mucosal, mesenteric lymph nodes (MLN), and the spleen (Fig. 8, *D–F*). Furthermore, intra-rectal delivery of DNP resulted in small increases in bacterial translocation that were aggravated by DAPK6 and alleviated by tunicamycin co-treatment (Fig. 8, *G–I*).

Discussion

Increased numbers of bacteria, including *E. coli*, in the mucosa and gut epithelium can characterize IBD (1). Many lines of evidence point to dysregulated mitochondrial function in cohorts of patients with IBD (6, 10). By juxtaposing these two putative etiological factors in enteric inflammation, we showed increased *E. coli* internalization and transcytosis across epithelia treated with the hydrogen ionophore, DNP, that uncouples oxidative phosphorylation (15). Mitochondria do not function in isolation; they couple to the ER. Indeed, dysregulation of the UPR (or ER stress) can contribute to gut inflammation (27); data in support of this have accumulated mostly from analyses of Paneth (24) and goblet cells (28). The importance of mitochondria–ER interaction in the transporting enterocyte (the majority of the gut surface area) to host defense is poorly appreciated. The findings herein suggest that mobilization of the ATF6-arm of the UPR via DAPK1-dependent autophagy results in killing of bacteria taken into the cell because of disrupted mitochondrial function, effectively reducing the barrier defect elicited by metabolic stress. Support for this conclusion comes from the use of a variety of human-derived cell lines, human biopsies, primary mouse organoids, and murine models. Although each model has its pros and cons, the demonstration of the major phenomenon of this research in four model systems, adds, we believe, validity to the findings.

Many stimuli implicated in IBD reactivation can result in dysfunctional mitochondria (5). For instance, NSAID use can elicit disease relapse in some patients with IBD (29), and NSAID enteropathy is characterized by abnormal epithelial mitochondrial structure (8, 9). Modeling mitochondrial dysfunction with DNP treatment provided evidence that targeted loss of mitochondrial function resulted in ROS-dependent internalization of bacteria by enteric epithelia (15).

An excessive UPR can lead to colitis (28), and an inability to mount a normal UPR response increases susceptibility to colitis (17). Here, the hypothesis that a UPR-ER stress response would exaggerate an epithelial barrier defect triggered by increased oxidative stress proved to be incorrect; reduced translocation and fewer viable intracellular bacteria occurred in epithelia treated with ER stressors. Also, the apoptosis that occurred with longer DNP + *E. coli* exposure (36 h) was reduced by tunicamycin, which would preserve epithelial barrier function. ER stress occurs in response to pathogens: bacterial, viral, and fungi. The demonstration that provocation of an ER stress response to counter the effect of epithelial internalization of commensal bacteria caused by mitochondrial dysfunction underscores that this is an important aspect of innate immunity when challenged with intracellular microbes.

Autophagy is important in host defense, where, for example, protection against colitis by outer membrane vesicles from *Bacteroides fragilis* requires ATG16L1-competent dendritic cells (30). Tunicamycin did not affect internalization of inert beads into DNP-treated epithelia but enhanced autophagy markers suggesting that the reduction in viable intracellular bacteria was because of reduced survival. In accordance, the protective effect of tunicamycin was lost in epithelia lacking the autophagy protein, ATG16L1. The threonine-to-alanine (T300A) ATG16L1 variant that increases the risk for Crohn's disease results in degradation of the protein (31), reducing autophagic capacity and leaving the individual vulnerable to pathogenic bacteria (32, 33). The equivalent mutation in the mouse (T316A) also targets Atg16l1 for destruction (31). Monolayers from colonoids of the *Atg16l1*^{T316A} knockin mouse not only had increased responses to DNP, as gauged by *E. coli* internalization but tunicamycin failed to reverse this event. These data support the view that the UPR via autophagy antagonizes the barrier defect evoked by perturbed mitochondrial function.

Given the significance of the colonic microbiota in IBD pathophysiology and that transporting enterocyte is the major constituent of the epithelium, we speculate that the impact of the ATG16L1^{T300A} mutation would be compounded in the context of reduced mitochondrial activity due to NSAID use or other stimuli (6). Furthermore, a cytoprotective effect of ATG16L1 in epithelial cells promoted mitochondrial homeostasis and prevented necroptosis (34). Collectively, these data suggest that the development of drugs that drive autophagy (35) or an appropriate UPR (ER stress) pathway would be of value in treating enteropathies (*e.g.* IBD) characterized by loss of epithelial barrier function, *i.e.* uptake and passage of commensal bacteria, pathobionts, and pathogens, due to perturbed mitochondrial function. In this context, the anti-colitic pro-drug thioguanine promoted autophagy in human colon-derived epithelial cell lines, limiting *Salmonella typhimurium* replication (36).

The balance of this mitochondria–ER–autophagy cross-talk would be central to cell health. Up-regulation of autophagy would prevent the effects of excessive ER stress, and in the short-term, it has the benefit of targeting internalized bacteria as a consequence of mitochondrial dysfunction. Contrarily, prolonged ER stress and/or autophagy would be detrimental and potentially of pathophysiological significance (37, 38).

Essentially the UPR is a three-pronged pathway, in which any one arm can dominate (39), such as the mobilization of Ire1/

Figure 5. ATF-6 mediates inhibition of the DNP effect. *A,* T84 cells treated with *E. coli* + DNP + tunicamycin show increased expression of ATF6 but not XBP1 or ATF4 (representative immunoblot; 16-h treatments; densitometry). *B,* treatment with ATF6α, but not ATF4 or XBP1, siRNA (*inset*, immunoblots showing siRNA knockdown of protein) prevents the ability of TM (10 μg/ml) to ablate the DNP (0.1 mM)-induced internalization of viable *E. coli* (10^6 cfu, strain HB101; 16 h) (one representative experiment of two experiments). *C,* immunoblotting of whole-cell extracts (representative of three blots) reveals increased phosphorylated JNK in TM + DNP-, but not *E. coli* only, treated T84 epithelial cells. *D,* co-treatment with the selective pharmacological inhibitor of JNK, SP600125 (40 nM), does not affect the TM suppression of DNP-evoked increases in viable intracellular *E. coli* in T84 epithelial cells (16 h). *E,* co-treatment with the selective IRE1 inhibitor (KIRA6, 600 nM) or PERK inhibitor (GSK2606414, 0.4 nM) did not affect DNP (0.1 mM, 16 h)-induced internalization of *E. coli* into T84 cells. *F,* increased autophagy as gauged by LC3-II protein expression observed in *E. coli* + DNP + TM-treated cells was not observed in T84 epithelia treated with siRNA against ATF6α. The inducer of autophagy, rapamycin (*Rapa*, 100 nM) is shown as a positive control (mean ± S.D.; *, $p < 0.05$ compared with control).

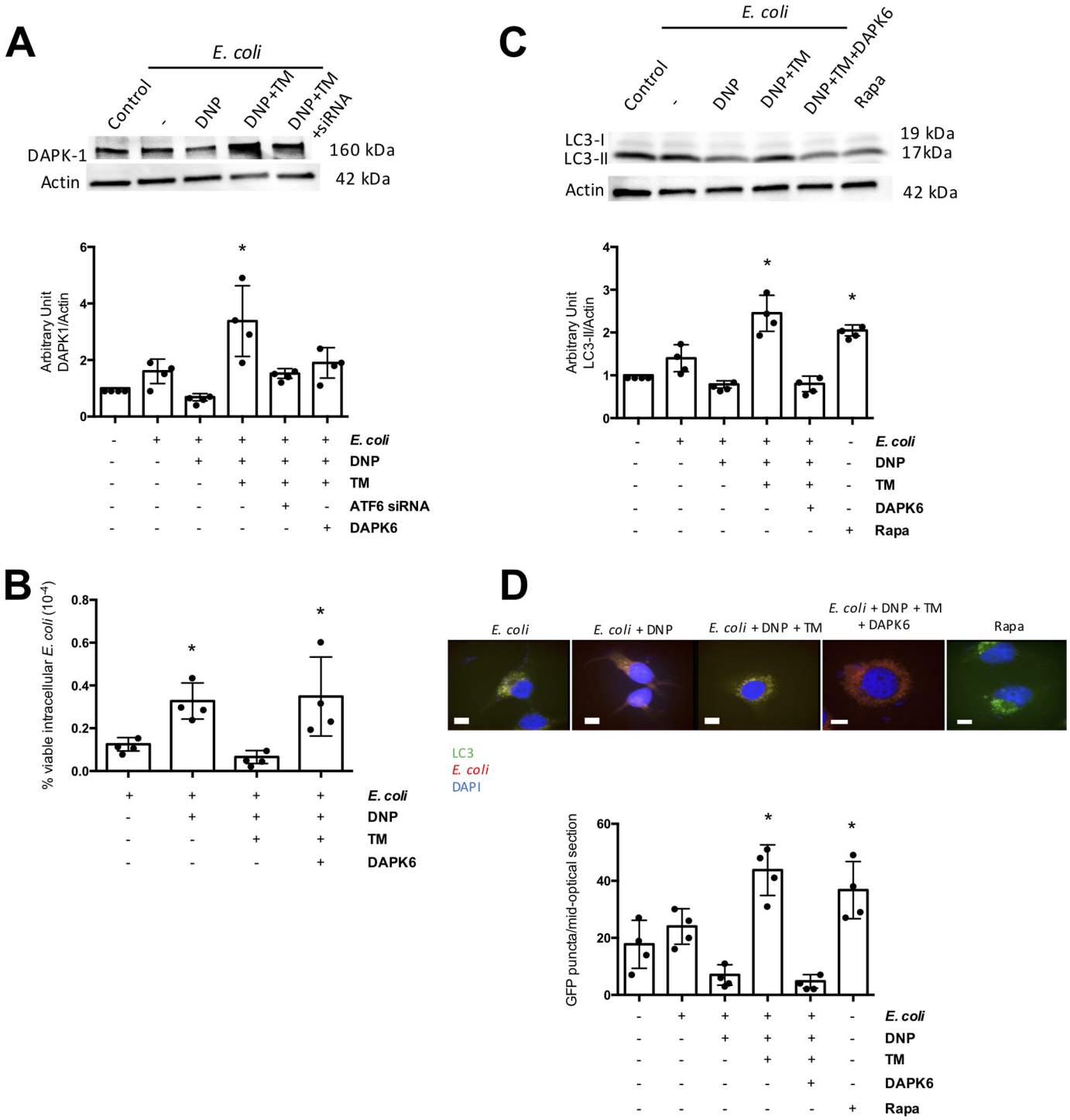

Figure 6. DAP kinase-1 is needed for tunicamycin inhibition of DNP-evoked decreased barrier function. *A,* immunoblotting of whole-cell extracts of wildtype or ATF6 siRNA (2 nM)-treated T84 epithelial cells exposed to *E. coli* + DNP (0.1 mM) and TM (10 μg/ml) for 4 h shows an ATF6-dependent increase in DAPK1 expression. *B,* TM antagonism of DNP-induced increases in viable intracellular *E. coli* (10^6 cfu, 16 h) by T84 cells was not observed in cells co-treated with the selective inhibitor of DAPK1, DAPK6 (10 μM). *C,* DAPK6 suppressed autophagy evoked as a consequence of *E. coli*-DNP + TM treatment as assessed by immunoblotting for LC3-II in T84 cells; *D,* enumeration of LC3-GFP$^+$ puncta formation in HeLa cells (mean ± S.D.; * and #, $p < 0.05$ compared with control and DNP, respectively).

Xbp1 signaling following bacterial infection or accumulation of Ire1α aggregates in *Atg16l1*$^{\Delta IEC}$ mice that may contribute to Crohn's disease-like ileitis (37). Molecular knockout and use of PERK, IRE1, and JNK-selective inhibitors indicated that tunicamycin abrogation of the DNP-induced epithelial barrier defect was dependent on the ATF6 arm of the UPR. Other studies support a beneficial role for Atf6 in limiting enteric inflammation: mutation in a protease resulting in reduced Atf6 activation increased susceptibility to DSS-induced colitis (data on bacterial translocation were not presented) (40); *Atf6*$^{-/-}$ mice display increased susceptibility to bacteria correlating with decreased autophagy in macrophages (41). Furthermore, IL-10

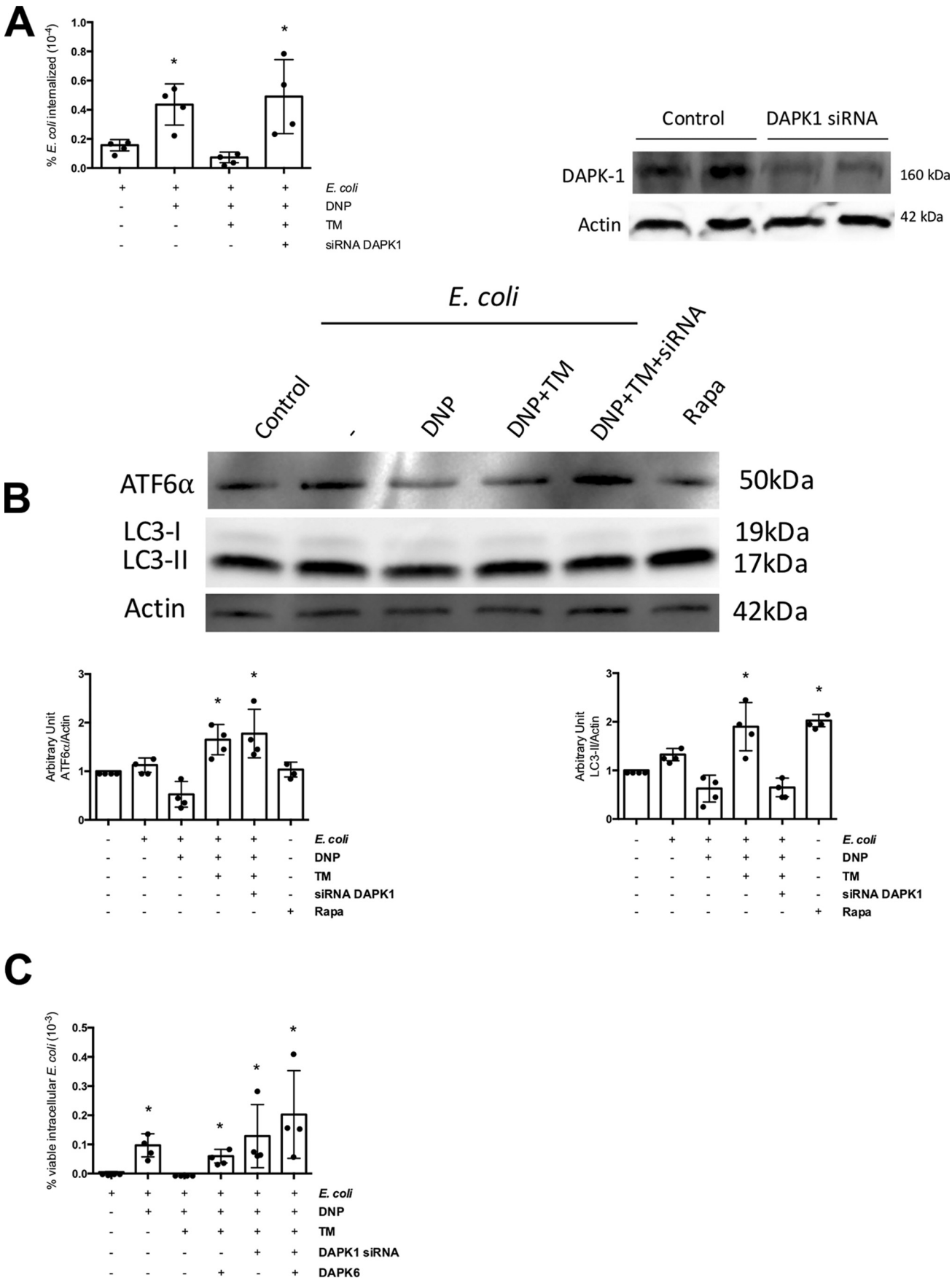
A
% E. coli internalized (10-4)
1.0
0.8
0.6
0.4
0.2
0.0
*
*
+ + + + E. coli
- + + + DNP
- - + + TM
- - - + siRNA DAPK1
Control
DAPK1 siRNA
DAPK-1
160 kDa
Actin
42 kDa
E. coli
Control
DNP
DNP+TM
DNP+TM+siRNA
Rapa
B
ATF6α
50kDa
LC3-I
LC3-II
19kDa
17kDa
Actin
42kDa
Arbitrary Unit ATF6α/Actin
3
2
1
0
- + + + + - E. coli
- - + + + - DNP
- - - + + - TM
- - - - + - siRNA DAPK1
- - - - - + Rapa
Arbitrary Unit LC3-II/Actin
- + + + + - E. coli
- - + + + - DNP
- - - + + - TM
- - - - + - siRNA DAPK1
- - - - - + Rapa
C
% viable intracellular E. coli (10-3)
0.5
0.4
0.3
0.2
0.1
0.0
+ + + + + + E. coli
- + + + + + DNP
- - + + + + TM
- - - - + + DAPK1 siRNA
- - - + - + DAPK6

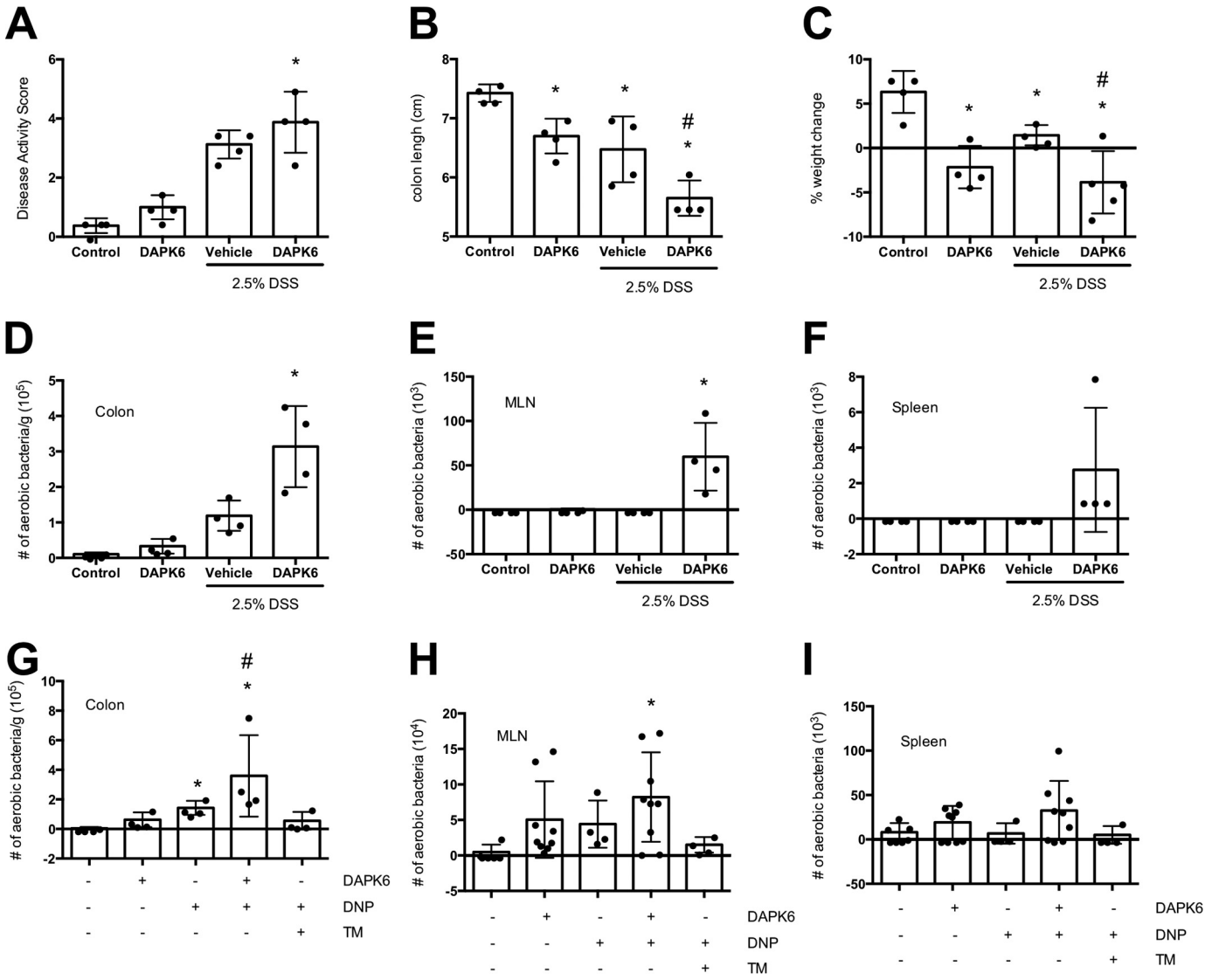

Figure 8. Systemic delivery of DAPK1 enhances bacterial translocation *in vivo*. Male C57Bl/6 mice were treated with 2.5% (w/v) DSS (~40 kDa) in their drinking water for 5 days (*A–F*). Additional mice received the DAPK1 inhibitor DAPK6 (20 μg/kg, i.p. daily). Mice were euthanized, and disease activity was assessed in the DSS-treated mice, and bacterial translocation into the colonic mucosa, MLN, and spleen was determined in all mice. *G–I,* male C57Bl/6 mice were intra-rectally administered DNP (3 mM) for 24 h. Additional mice received DAPK6 (20 μg/kg, i.p. daily) ± TM (20 μg/kg, i.p. daily). Mice were euthanized, and bacterial translocation into the colonic mucosa, MLN, and spleen was determined in all mice (mean ± S.D.; * and #, $p < 0.05$ compared with control and DSS or DNP, respectively).

can exert an anti-inflammatory effect via inhibition of TNFα-induced nuclear translocation of ATF6 (20).

ATF6 regulates DAPK1 synthesis (26), which can phosphorylate Beclin-1 to induce autophagy (42) and stimulate trafficking of Atg9-containing vesicles for autophagosome formation in response to starvation (43); *dapk1*$^{-/-}$ fibroblasts display less autophagy following tunicamycin treatment (44). Although preliminary, a polymorphism in the *DAPK1* gene is reported in some patients with Crohn's disease (45). Noting that ATF6 siRNA-treated epithelia had reduced DAPK1 expression, it was determined that tunicamycin failed to ablate the DNP-evoked increase in viable intracellular *E. coli* in epithelia treated with a DAPK1-selective inhibitor, DAPK6, or DAPK1 siRNA, correlating with reduced autophagy. Moreover, treatment of mice with 2.5% DSS resulted in bacterial translocation into the colonic mucosa and MLNs that was significantly increased by DAPK6 co-treatment. Similarly, bacterial translocation (*i.e.* barrier defect) evoked by intra-rectal DNP (which was reduced by tunicamycin co-treatment) was enhanced by systemic delivery of DAPK6.

There is an elegance in assessing a single variable in an experimental system; however, the coordinated activity of intracellu-

Figure 7. Knockdown of DAPK1 blocks tunicamycin inhibition of DNP-evoked decreased barrier function. *A,* DAPK1 knockdown with siRNA (40 pM) ablates the ability of the ER stressor TM (10 μg/ml) to reduce the number of viable intracellular *E. coli* (HB101, 10^6 CFU) in T84 epithelia evoked by exposure to DNP (0.1 mM; 16 h). *B,* expression of ATF6α and LC3-I and LC3-II as indicators of autophagy was analyzed by immunoblotting whole T84 cell extracts (± DAPK1 siRNA) 4 h after treatment with DNP, TM of DNP + TM. Rapamycin (*Rapa*; 100 nM) was used as a positive control to induce autophagy. *C,* co-treatment of T84 cells with DAPK1 siRNA and the inhibitor DAPK6 (10 μM) while blocking the effect of TM was not statistically significantly different from either agent alone (mean ± S.D.; *, $p < 0.05$ compared with control).

lar signaling cascades regulates cell and tissue function. By defining an ATF6–to–DAPK1–to–autophagy (and apoptosis) pathway, we define how the UPR can preserve epithelial barrier function when faced with deranged mitochondrial function. The implications of this could be wide-ranging. In the context of IBD, the effect of reduced activity or the loss of ATG16L1 affects not only macrophages, goblet cells, and Paneth cells but the transporting enterocyte as well, negating the value of mobilizing ATF6 to counter the transcellular passage of microbes across metabolically-stressed epithelia. It will be important to address how the mitochondria–to–ATF6–DAPK1–autophagy interaction is impacted by other molecules that control epithelia–microbe interaction (*e.g.* NOD proteins, NF$\kappa\beta$, and the inflammasome (38, 46, 47)). For instance, cells devoid of NOD2 are more sensitive to DNP-induced barrier defects (48), and reduced epithelia autophagy due to knockout of the amino acid sensor *GCN2* (a starvation model analogous to DNP exposure) was linked to ROS generation, inflammasome activation, and intestinal inflammation (47).

Epithelial–microbial interactions are at the nexus of IBD. Having defined a molecular pathway in the transporting enterocyte by which mobilization of the UPR abolishes the epithelial transcellular permeability defect (*i.e.* bacteria uptake and passage) in metabolically-stressed cells, we suggest that this is critical in gut homeostasis. Controlled ER stress, via autophagy, rescues the enterocyte from the loss of barrier function, as measured by bacterial transcytosis, caused by uncoupling oxidative phosphorylation. Reciprocally, the pathophysiological consequences of compromised autophagy or ER stress (both susceptibility traits for IBD) is compounded by perturbed mitochondrial function that drives the internalization of commensal bacteria by the epithelium, the enhanced survival of which could be a significant pro-inflammatory stimulus.

Experimental procedures

Human biopsies and murine colonoids

Human colonic biopsies were obtained from two healthy men and five women (mean age 78 years) at the Gastroenterology Department, University Hospital in Linköping. The Regional Committee of human ethics approved the study, and all subjects gave informed consent.

Mice with the *Atg16l1*^{T316A} knockin gene (from M. van Lookeren Champagne, Genentech, San Francisco) were housed in standard conditions under protocol AC13-0015 (Animal Care Committee, University of Calgary). Experiments conformed to Canadian guidelines on animals in research. Colonic crypts were isolated (49), cultured in IntestiCult™ organoid growth medium (Stemcell, BC Canada), and monolayers grown on filter supports (50). *E. coli* HB101 was grown overnight in Luria-Bertani (LB) broth, and 10^7 colony-forming units (cfu) were added to the luminal aspect of filter-grown epithelia, and bacterial translocation was assessed by sampling medium from the basal compartment of the culture well.

Reagents

DNP, tunicamycin, rapamycin, 3-MA, brefeldin-A, thapsigargin, and FITC-4-kDa dextran were from Sigma. SP600125 (JNK inhibitor), DAPK6 (DAPK1 inhibitor), and GSK2606414 (PERK inhibitor) were all from Tocris Bioscience (Bristol, UK), and KIRA6 (IRE-1 inhibitor) was from EMD Millipore (Darmstadt, Germany). Green-yellow latex beads, *E. coli* F12 fluorescent BioParticles, and DAPI were from Molecular Probes (Eugene, OR). The *E. coli* strain HB101 was provided by Dr. Philip M. Sherman (Hospital for Sick Children, University of Toronto, Ontario, Canada).

Ussing chambers studies

Human colonic biopsies were mounted in Ussing chambers (1.8-mm^2 surface area) (51). Live non-pathogenic GFP-labeled *E. coli* (HS strain; 10^8 cfu/ml) (52) were added to the mucosal side of the tissue with DNP (0.1 mM) ± tunicamycin (10 μg/ml) or rapamycin (100 nM). Additional biopsies from the same individual bathed in Krebs buffer only served as controls. All conditions were performed in duplicate biopsies. After 3 h, serosal buffers were collected, and fluorescence was measured at 488 nm in VICTOR™ *X3* multileader plate reader (PerkinElmer Life Sciences, Sweden). Other biopsies were homogenized in 200 μl of RIPA buffer, serially diluted, plated onto LB agar, cultured under aerobic conditions (~16 h, 37 °C), and colony-forming units counted.

Cell culture, bacterial translocation, and intracellular viable bacteria

The T84, CaCo2, and HCT116 human colonic epithelial cell lines and the cervical epithelial HeLa cell line were maintained as described (15) (T84 *NOD2*$^{-/-}$ cells were used generated via shRNA (48)). Cells (10^6/ml) were seeded into 12-well plates and used at ~70% confluence based on phase-contrast microscopy or onto 3.0-μm porous filter supports and cultured for 7 days until electrically confluent (T84 >1000 ohms·cm^2; HT-29 >300 ohms·cm^2) (15). *E. coli* HB101 was grown overnight in LB broth, and 10^6 cfu were added to the epithelium (luminal aspect of filter-grown polarized preparations). The intracellular viable bacteria number was assessed by killing extracellular bacteria with 200 μg/ml gentamicin (2 h), followed by enterocyte lysis (0.1% Triton X-100), and culturing serial dilutions of the cell extract. Bacterial translocation was assessed by sampling the medium from the basolateral compartment of filter-grown epithelia (15). All drugs were added simultaneously with the *E. coli* and were tested (at the doses used) for bacteriostatic and bactericidal effects.

TUNEL assay

Apoptotic cells were detected by TUNEL using ApopTag® in situ apoptosis detection kits (EDM Millipore).

Epithelial paracellular permeability

TER across filter-grown T84 cell monolayers was recorded at time 0 and 16 h later using a voltmeter and matched electrodes (Millicell-ERS, Millipore, Bedford, MA). Data are presented as a percentage of pretreatment TER value.

Following treatment, FITC-dextran (80 μg/ml, 4 kDa) in fresh culture medium was added to the apical surface of filter-grown T84 cell monolayers for 4 h at 37 °C. Samples were collected from the basolateral well of the chamber, and fluores-

cence was read at excitation (427 nm) and emission (536 nm) wavelengths.

Cell bioenergetics

The oxygen consumption rate and extracellular acidification rate were measured using a Seahorse XF-24 metabolic flux analyzer (Seahorse Bioscience, North Billerica, MA).

GFP-LC3 autophagy detection

HeLa cells expressing LC3-GFP (53) were used, and images were captured by confocal microscopy. ImageJ was used for unbiased LC3 puncta analysis in the mid-optical section of live cells. Cells were identified as a region with greater than 1 S.D. higher intensity MAP2 or HA stain than the mean intensity for that individual image. A punctum was identified as a region of LC3 stain that was more than 2 S.D. brighter than the individual image mean. All LC3 puncta larger than 0.1 μm within the MAP2 or HA stain were included in the analysis (smaller puncta are outside the size range of phagophores/autophagosomes at 0.2–10 μm).

siRNA

T84 cells in suspension (2×10^6/ml) ± ATG16L1 (20 nM), ATF6α (1000 nM), IRE1β (100 nM), PERK (1000 nM), or DAPK1 (40 nM) siRNA Silencer® pre-designed (Inventoried) siRNA (Thermo Fisher Scientific) were electroporated using the AMAXA electroporation device and then seeded into plates. Twenty four (ATF6α, IRE1β, and PERK) or 48 h (ATG16L1 and DAPK1) later, cells were rinsed and used in experiments (gene knockdown confirmed by immunoblotting).

ATG16L1 knockout

CRISPR-Cas9 methodology (54) was used to knockout *ATG16L1* in the human HCT116 epithelial cell line. A gRNA target region (5′-ATGAGTATCCACATTGTCCT-3′) was identified using the crispr.mit.edu website (Zhang laboratory at MIT), cloned into pSpCas9(BB)-2A-Puro plasmid (Addgene plasmid 48139), and verified by sequencing. HCT116 cells were grown to 50% confluence in 100-mm tissue culture dishes and transfected with 2 μg of pSpCas9(gRNA)-2A-Puro plasmid using 20 μl of polyethyleneimine (Polysciences, Warrington, PA). Successfully transfected cells were selected 24 h later with 3 μg/ml puromycin. Limiting dilution was used to create clonal cell lines, of which the identity and knockout of *ATG16L1* were verified by sequencing and immunoblotting for ATG16L1.

Latex bead phagocytosis

T84 cells plated in chamber slides (10^5/ml) at ~70% confluence were treated with FluoSpheres® carboxylate (1 μm, yellow-green (505/515), 10^5/ml) or killed *E. coli* F12 fluorescent bioparticles (10^6/ml) (both from Thermo Fisher Scientific). Samples were analyzed by fluorescent microscopy and flow cytometry.

Protein immunodetection

Standard immunoblotting protocols were used to detect GRP78, ATF6α (Santa Cruz Biotechnology) (55), ATG16L1 (56), DAPK1 (57), LC3-II (58), sXBP1 (59), ATF4 (60), and p-JNK (61) (Cell Signaling Technology) in T84, CaCo2, and HCT116 epithelium using primary antibodies at 1:1000 dilution.

In vivo bacterial translocation

Data from mouse models have limitations when extrapolating to humans; indeed, there is no model of IBD, but there are useful models of colitis for pre-clinical investigation. Bearing this in mind, colitis was induced in 7–9-week-old male C57Bl/6 mice (Charles River Laboratories, Senneville, Quebec, Canada) by 2.5% (w/v) DSS (~40 kDa) in drinking water for 5 days (an often used model (15)) ± daily DAPK6 (20 μg/kg; i.p.). At necropsy, a disease activity score based on body weight, colon length, and the animal's macroscopic appearance, colon, and stool was calculated. Two-cm pieces of colon, the mesenteric lymph nodes, and spleen were excised, rinsed in gentamicin (200 μg/ml), homogenized, serial dilution plated onto blood agar (37 °C, 24 h), and cfu counted.

Other mice received DNP (3 mM in 100 μl PBS) intrarectally (13) ± DAPK6 or tunicamycin (20 μg/kg; i.p.), and 24 h later tissues were processed, and bacterial translocation was assessed.

Statistical analysis

Data are means ± S.D. Multiple group comparisons were performed by one-way analysis of variance, followed by pairwise post hoc tests, with $p < 0.05$ as a level of statistical significant difference.

Author contributions—F. L. and D. M. M. conceptualization; F L., A. S., J. L. R., N. M., A. A. R., A. W., C. B., M. D., Y. A., M. C., N. P., J. M. R., J. D. S., and D. M. M. data curation; F. L., Å. V. K., A. S., J. L. R., A. W., C. B., Y. A., M. C., W. M., H. J., D. J. P., and J. D. S. formal analysis; F. L. and D. M. M. validation; F. L., Å. V. K., N. M., A. A. R., A. W., Y. A., W. M., S. E. G., H. J., D. J. P., J. D. S., and D. M. M. investigation; F. L., Å. V. K., C. B., M. D., R. v. D., Y. A., M. C., W. M., H. J., and J. D. S. methodology; F. L. writing-original draft; A. W. and D. M. M. project administration; J. M. R., S. E. G., J. D. S., and D. M. M. funding acquisition; D. M. M. resources; D. M. M. supervision; D. M. M. writing-review and editing.

Acknowledgments—Facilities and expertise provided by the Live Cell Imaging Suite, Snyder Institute for Chronic Disease at the Cumming School of Medicine (University of Calgary), are gratefully acknowledged.

References

1. Elliott, T. R., Hudspith, B. N., Wu, G., Cooley, M., Parkes, G., Quiñones, B., Randall, L., Mandrell, R. E., Fagerquist, C. K., Brostoff, J., Rayment, N. B., Boussioutas, A., Petrovska, L., and Sanderson, J. D. (2013) Quantification and characterization of mucosa-associated and intracellular *Escherichia coli* in inflammatory bowel disease. *Inflamm. Bowel Dis.* **19,** 2326–2338 CrossRef Medline
2. Darfeuille-Michaud, A., Boudeau, J., Bulois, P., Neut, C., Glasser, A. L., Barnich, N., Bringer, M. A., Swidsinski, A., Beaugerie, L., and Colombel, J. F. (2004) High prevalence of adherent-invasive *Escherichia coli* associated with ileal mucosa in Crohn's disease. *Gastroenterology* **127,** 412–421 CrossRef Medline
3. Keita, A. V., Salim, S. Y., Jiang, T., Yang, P. C., Franzén, L., Söderkvist, P., Magnusson, K. E., and Söderholm, J. D. (2008) Increased uptake of non-

pathogenic *E. coli* via the follicle-associated epithelium in longstanding ileal Crohn's disease. *J. Pathol.* **215,** 135–144 CrossRef Medline

4. Moussata, D., Goetz, M., Gloeckner, A., Kerner, M., Campbell, B., Hoffman, A., Biesterfeld, S., Flourie, B., Saurin, J. C., Galle, P. R., Neurath, M. F., Watson, A. J., and Kiesslich, R. (2011) Confocal laser endomicroscopy is a new imaging modality for recognition of intramucosal bacteria in inflammatory bowel disease *in vivo*. *Gut* **60,** 26–33 CrossRef Medline
5. Russell, R. K., Drummond, H. E., Nimmo, E. R., Anderson, N. H., Noble, C. L., Wilson, D. C., Gillett, P. M., McGrogan, P., Hassan, K., Weaver, L. T., Bisset, W. M., Mahdi, G., and Satsangi, J. (2006) Analysis of the influence of OCTN1/2 variants within the IBD5 locus on disease susceptibility and growth indices in early onset inflammatory bowel disease. *Gut* **55,** 1114–1123 Medline
6. Schoultz, I., Söderholm, J. D., and McKay, D. M. (2011) Is metabolic stress a common denominator in inflammatory bowel disease? *Inflamm. Bowel Dis.* **17,** 2008–2018 CrossRef Medline
7. Klein, A., and Eliakim, R. (2010) Non-steroidal anti-inflammatory drugs and inflammatory bowel disease. *Pharmaceuticals* **3,** 1084–1092 CrossRef Medline
8. Somasundaram, S., Sigthorsson, G., Simpson, R. J., Watts, J., Jacob, M., Tavares, I. A., Rafi, S., Roseth, A., Foster, R., Price, A. B., Wrigglesworth, J. M., and Bjarnason, I. (2000) Uncoupling of intestinal mitochondrial oxidative phosphorylation and inhibition of cyclooxygenase are required for the development of NSAID-enteropathy in the rat. *Aliment. Pharmacol. Ther.* **14,** 639–650 CrossRef Medline
9. Schoultz, I., McKay, C. M., Graepel, R., Phan, V. C., Wang, A., Söderholm, J., and McKay, D. M. (2012) Indomethacin-induced translocation of bacteria across enteric epithelia is reactive oxygen species-dependent and reduced by vitamin C. *Am. J. Physiol. Gastrointest. Liver Physiol.* **303,** G536–G545 CrossRef Medline
10. Rath, E., and Haller, D. (2012) Mitochondria at the interface between danger signaling and metabolism: role of unfolded protein responses in chronic inflammation. *Inflamm. Bowel Dis.* **18,** 1364–1377 CrossRef Medline
11. Khor, B., Gardet, A., and Xavier, R. J. (2011) Genetics and pathogenesis of inflammatory bowel disease. *Nature* **474,** 307–317 CrossRef Medline
12. Odenwald, M. A., and Turner, J. R. (2017) The intestinal epithelial barrier: a therapeutic target? *Nat. Rev. Gastroenterol. Hepatol.* **14,** 9–21 CrossRef Medline
13. Nazli, A., Yang, P. C., Jury, J., Howe, K., Watson, J. L., Söderholm, J. D., Sherman, P. M., Perdue, M. H., and McKay, D. M. (2004) Epithelia under metabolic stress perceive commensal bacteria as a threat. *Am. J. Pathol.* **164,** 947–957 CrossRef Medline
14. Lewis, K., Lutgendorff, F., Phan, V., Söderholm, J. D., Sherman, P. M., and McKay, D. M. (2010) Enhanced translocation of bacteria across metabolically stressed epithelia is reduced by butyrate. *Inflamm. Bowel Dis.* **16,** 1138–1148 CrossRef Medline
15. Wang, A., Keita, Å. V., Phan, V., McKay, C. M., Schoultz, I., Lee, J., Murphy, M. P., Fernando, M., Ronaghan, N., Balce, D., Yates, R., Dicay, M., Beck, P. L., MacNaughton, W. K., Söderholm, J. D., and McKay, D. M. (2014) Targeting mitochondria-derived reactive oxygen species to reduce epithelial barrier dysfunction and colitis. *Am. J. Pathol.* **184,** 2516–2527 CrossRef Medline
16. Marchi, S., Patergnani, S., and Pinton, P. (2014) The endoplasmic reticulum-mitochondria connection: one touch, multiple functions. *Biochim. Biophys. Acta* **1837,** 461–469 CrossRef Medline
17. Kaser, A., Lee, A. H., Franke, A., Glickman, J. N., Zeissig, S., Tilg, H., Nieuwenhuis, E. E., Higgins, D. E., Schreiber, S., Glimcher, L. H., and Blumberg, R. S. (2008) XBP1 links ER stress to intestinal inflammation and confers genetic risk for human inflammatory bowel disease. *Cell* **134,** 743–756 CrossRef Medline
18. Zhang, H. S., Chen, Y., Fan, L., Xi, Q. L., Wu, G. H., Li, X. X., Yuan, T. L., He, S. Q., Yu, Y., Shao, M. L., Liu, Y., Bai, C. G., Ling, Z. Q., Li, M., Liu, Y., and Fang, J. (2015) The endoplasmic reticulum stress sensor IRE1α in intestinal epithelial cells is essential for protecting against colitis. *J. Biol. Chem.* **290,** 15327–15336 CrossRef Medline
19. Cao, S. S., Zimmermann, E. M., Chuang, B. M., Song, B., Nwokoye, A., Wilkinson, J. E., Eaton, K. A., and Kaufman, R. J. (2013) The unfolded protein response and chemical chaperones reduce protein misfolding and colitis in mice. *Gastroenterology* **144,** 989–1000 CrossRef Medline
20. Shkoda, A., Ruiz, P. A., Daniel, H., Kim, S. C., Rogler, G., Sartor, R. B., and Haller, D. (2007) Interleukin-10 blocked endoplasmic reticulum stress in intestinal epithelial cells: impact on chronic inflammation. *Gastroenterology* **132,** 190–207 CrossRef Medline
21. Ling, Y. H., Li, T., Perez-Soler, R., and Haigentz, M., Jr. (2009) Activation of ER stress and inhibition of EGFR *N*-glycosylation by tunicamycin enhances susceptibility of human non-small cell lung cancer cells to erlotinib. *Cancer Chemother. Pharmacol.* **64,** 539–548 CrossRef Medline
22. Shen, T., Li, Y., Chen, Z., Liang, S., Guo, Z., Wang, P., Wu, Q., Ba, G., and Fu, Q. (2017) CHOP negatively regulates Polo-like kinase 2 expression via recruiting C/EBPα to the upstream-promoter in human osteosarcoma cell line during ER stress. *Int. J. Biochem. Cell Biol.* **89,** 207–215 CrossRef Medline
23. Drion, C. M., Borm, L. E., Kooijman, L., Aronica, E., Wadman, W. J., Hartog, A. F., van Vliet, E. A., and Gorter, J. A. (2016) Effects of rapamycin and curcumin treatment on the development of epilepsy after electrically induced status epilepticus in rats. *Epilepsia* **57,** 688–697 CrossRef Medline
24. Adolph, T. E., Tomczak, M. F., Niederreiter, L., Ko, H. J., Böck, J., Martinez-Naves, E., Glickman, J. N., Tschurtschenthaler, M., Hartwig, J., Hosomi, S., Flak, M. B., Cusick, J. L., Kohno, K., Iwawaki, T., Billmann-Born, S., *et al.* (2013) Paneth cells as a site of origin for intestinal inflammation. *Nature* **503,** 272–276 CrossRef Medline
25. Grootjans, J., Kaser, A., Kaufman, R. J., and Blumberg, R. S. (2016) The unfolded protein response in immunity and inflammation. *Nat. Rev. Immunol.* **16,** 469–484 CrossRef Medline
26. Gade, P., Kimball, A. S., DiNardo, A. C., Gangwal, P., Ross, D. D., Boswell, H. S., Keay, S. K., and Kalvakolanu, D. V. (2016) Death-associated protein kinase-1 expression and autophagy in chronic lymphocytic leukemia are dependent on activating transcription factor-6 and CCAAT/enhancer-binding protein-β. *J. Biol. Chem.* **291,** 22030–22042 CrossRef Medline
27. Bogaert, S., De Vos, M., Olievier, K., Peeters, H., Elewaut, D., Lambrecht, B., Pouliot, P., and Laukens, D. (2011) Involvement of endoplasmic reticulum stress in inflammatory bowel disease: a different implication for colonic and ileal disease? *PLoS One* **6,** e25589 CrossRef Medline
28. Heazlewood, C. K., Cook, M. C., Eri, R., Price, G. R., Tauro, S. B., Taupin, D., Thornton, D. J., Png, C. W., Crockford, T. L., Cornall, R. J., Adams, R., Kato, M., Nelms, K. A., Hong, N. A., Florin, T. H., Goodnow, C. C., and McGuckin, M. A. (2008) Aberrant mucin assembly in mice causes endoplasmic reticulum stress and spontaneous inflammation resembling ulcerative colitis. *PLoS Med.* **5,** e54 CrossRef Medline
29. Kvasnovsky, C. L., Aujla, U., and Bjarnason, I. (2015) Nonsteroidal anti-inflammatory drugs and exacerbations of inflammatory bowel disease. *Scand. J. Gastroenterol.* **50,** 255–263 CrossRef Medline
30. Chu, H., Khosravi, A., Kusumawardhani, I. P., Kwon, A. H., Vasconcelos, A. C., Cunha, L. D., Mayer, A. E., Shen, Y., Wu, W. L., Kambal, A., Targan, S. R., Xavier, R. J., Ernst, P. B., Green, D. R., McGovern, D. P., Virgin, H. W., and Mazmanian, S. K. (2016) Gene-microbiota interactions contribute to the pathogenesis of inflammatory bowel disease. *Science* **352,** 1116–1120 CrossRef Medline
31. Murthy, A., Li, Y., Peng, I., Reichelt, M., Katakam, A. K., Noubade, R., Roose-Girma, M., DeVoss, J., Diehl, L., Graham, R. R., and van Lookeren Campagne, M. (2014) A Crohn's disease variant in Atg16l1 enhances its degradation by caspase 3. *Nature* **506,** 456–462 CrossRef Medline
32. Lassen, K. G., Kuballa, P., Conway, K. L., Patel, K. K., Becker, C. E., Peloquin, J. M., Villablanca, E. J., Norman, J. M., Liu, T. C., Heath, R. J., Becker, M. L., Fagbami, L., Horn, H., Mercer, J., Yilmaz, O. H., *et al.* (2014) Atg16L1 T300A variant decreases selective autophagy resulting in altered cytokine signaling and decreased antibacterial defense. *Proc. Natl. Acad. Sci. U.S.A.* **111,** 7741–7746 CrossRef Medline
33. Sadaghian Sadabad, M., Regeling, A., de Goffau, M. C., Blokzijl, T., Weersma, R. K., Penders, J., Faber, K. N., Harmsen, H. J., and Dijkstra, G. (2015) The ATG16L1-T300A allele impairs clearance of pathosymbionts in the inflamed ileal mucosa of Crohn's disease patients. *Gut* **64,** 1546–1552 CrossRef Medline

34. Matsuzawa-Ishimoto, Y., Shono, Y., Gomez, L. E., Hubbard-Lucey, V. M., Cammer, M., Neil, J., Dewan, M. Z., Lieberman, S. R., Lazrak, A., Marinis, J. M., Beal, A., Harris, P. A., Bertin, J., Liu, C., Ding, Y., van den Brink, M. R. M., and Cadwell, K. (2017) Autophagy protein ATG16L1 prevents necroptosis in the intestinal epithelium. *J. Exp. Med.* **214,** 3687–3705 CrossRef Medline
35. Kuo, S. Y., Castoreno, A. B., Aldrich, L. N., Lassen, K. G., Goel, G., Dančík, V., Kuballa, P., Latorre, I., Conway, K. L., Sarkar, S., Maetzel, D., Jaenisch, R., Clemons, P. A., Schreiber, S. L., Shamji, A. F., and Xavier, R. J. (2015) Small-molecule enhancers of autophagy modulate cellular disease phenotypes suggested by human genetics. *Proc. Natl. Acad. Sci. U.S.A.* **112,** E4281–E4287 CrossRef Medline
36. Oancea, I., Movva, R., Das, I., Aguirre de Cárcer, D., Schreiber, V., Yang, Y., Purdon, A., Harrington, B., Proctor, M., Wang, R., Sheng, Y., Lobb, M., Lourie, R., Ó Cuív, P., Duley, J. A., Begun, J., and Florin, T. H. (2017) Colonic microbiota can promote rapid local improvement of murine colitis by thioguanine independently of T lymphocytes and host metabolism. *Gut* **66,** 59–69 CrossRef Medline
37. Tschurtschenthaler, M., Adolph, T. E., Ashcroft, J. W., Niederreiter, L., Bharti, R., Saveljeva, S., Bhattacharyya, J., Flak, M. B., Shih, D. Q., Fuhler, G. M., Parkes, M., Kohno, K., Iwawaki, T., Janneke van der Woude, C., Harding, H. P., *et al.* (2017) Defective ATG16L1-mediated removal of IRE1α drives Crohn's disease-like ileitis. *J. Exp. Med.* **214,** 401–422 CrossRef Medline
38. Diamanti, M. A., Gupta, J., Bennecke, M., De Oliveira, T., Ramakrishnan, M., Braczynski, A. K., Richter, B., Beli, P., Hu, Y., Saleh, M., Mittelbronn, M., Dikic, I., and Greten, F. R. (2017) IKKα controls ATG16L1 degradation to prevent ER stress during inflammation. *J. Exp. Med.* **214,** 423–437 CrossRef Medline
39. Yamamoto, K., Yoshida, H., Kokame, K., Kaufman, R. J., and Mori, K. (2004) Differential contributions of ATF6 and XBP1 to the activation of endoplasmic reticulum stress-responsive cis-acting elements ERSE, UPRE and ERSE-II. *J. Biochem.* **136,** 343–350 CrossRef Medline
40. Brandl, K., Rutschmann, S., Li, X., Du, X., Xiao, N., Schnabl, B., Brenner, D. A., and Beutler, B. (2009) Enhanced sensitivity to DSS colitis caused by a hypomorphic Mbtps1 mutation disrupting the ATF6-driven unfolded protein response. *Proc. Natl. Acad. Sci. U.S.A.* **106,** 3300–3305 CrossRef Medline
41. Gade, P., Ramachandran, G., Maachani, U. B., Rizzo, M. A., Okada, T., Prywes, R., Cross, A. S., Mori, K., and Kalvakolanu, D. V. (2012) An IFN-γ-stimulated ATF6-C/EBP-β-signaling pathway critical for the expression of death associated protein kinase 1 and induction of autophagy. *Proc. Natl. Acad. Sci. U.S.A.* **109,** 10316–10321 CrossRef Medline
42. Zalckvar, E., Berissi, H., Eisenstein, M., and Kimchi, A. (2009) Phosphorylation of Beclin 1 by DAP-kinase promotes autophagy by weakening its interactions with Bcl-2 and Bcl-XL. *Autophagy* **5,** 720–722 CrossRef Medline
43. Tang, H. W., Liao, H. M., Peng, W. H., Lin, H. R., Chen, C. H., and Chen, G. C. (2013) Atg9 interacts with dTRAF2/TRAF6 to regulate oxidative stress–induced JNK activation and autophagy induction. *Dev. Cell* **27,** 489–503 CrossRef Medline
44. Gozuacik, D., Bialik, S., Raveh, T., Mitou, G., Shohat, G., Sabanay, H., Mizushima, N., Yoshimori, T., and Kimchi, A. (2008) DAP-kinase is a mediator of endoplasmic reticulum stress–induced caspase activation and autophagic cell death. *Cell Death Differ.* **15,** 1875–1886 CrossRef Medline
45. Kaur, M., Panikkath, D., Yan, X., Liu, Z., Berel, D., Li, D., Vasiliauskas, E. A., Ippoliti, A., Dubinsky, M., Shih, D. Q., Melmed, G. Y., Haritunians, T., Fleshner, P., Targan, S. R., and McGovern, D. P. (2016) Perianal Crohn's disease is associated with distal colonic disease, stricturing disease behavior, IBD-associated serologies and genetic variation in the JAK-STAT pathway. *Inflamm. Bowel Dis.* **22,** 862–869 CrossRef Medline
46. Keestra-Gounder, A. M., Byndloss, M. X., Seyffert, N., Young, B. M., Chávez-Arroyo, A., Tsai, A. Y., Cevallos, S. A., Winter, M. G., Pham, O. H., Tiffany, C. R., de Jong, M. F., Kerrinnes, T., Ravindran, R., Luciw, P. A., McSorley, S. J., Bäumler, A. J., and Tsolis, R. M. (2016) NOD1 and NOD2 signalling links ER stress with inflammation. *Nature* **532,** 394–397 CrossRef Medline
47. Ravindran, R., Loebbermann, J., Nakaya, H. I., Khan, N., Ma, H., Gama, L., Machiah, D. K., Lawson, B., Hakimpour, P., Wang, Y. C., Li, S., Sharma, P., Kaufman, R. J., Martinez, J., and Pulendran, B. (2016) The amino acid sensor GCN2 controls gut inflammation by inhibiting inflammasome activation. *Nature* **531,** 523–527 CrossRef Medline
48. Saxena, A., Lopes, F., Poon, K. K. H., and McKay, D. M. (2017) Absence of the NOD2 protein renders epithelia more susceptible to barrier dysfunction due to mitochondrial dysfunction. *Am. J. Physiol. Gastrointest. Liver Physiol.* **313,** G26–G38 CrossRef Medline
49. Yui, S., Nakamura, T., Sato, T., Nemoto, Y., Mizutani, T., Zheng, X., Ichinose, S., Nagaishi, T., Okamoto, R., Tsuchiya, K., Clevers, H., and Watanabe, M. (2012) Functional engraftment of colon epithelium expanded *in vitro* from a single adult Lgr5(+) stem cell. *Nat. Med.* **18,** 618–623 CrossRef Medline
50. Fernando, E. H., Dicay, M., Stahl, M., Gordon, M. H., Vegso, A., Baggio, C., Alston, L., Lopes, F., Baker, K., Hirota, S., McKay, D. M., Vallance, B., and MacNaughton, W. K. (2017) A simple, cost-effective method for generating murine colonic 3D enteroids and 2D monolayers for studies of primary epithelial cell function. *Am. J. Physiol. Gastrointest. Liver Physiol.* **313,** G467–G475 CrossRef Medline
51. Wallon, C., Braaf, Y., Wolving, M., Olaison, G., and Söderholm, J. D. (2005) Endoscopic biopsies in Ussing chambers evaluated for studies of macromolecular permeability in the human colon. *Scand. J. Gastroenterol.* **40,** 586–595 CrossRef Medline
52. Keita, A. V., Gullberg, E., Ericson, A. C., Salim, S. Y., Wallon, C., Kald, A., Artursson, P., and Söderholm, J. D. (2006) Characterization of antigen and bacterial transport in the follicle-associated epithelium of human ileum. *Lab. Invest.* **86,** 504–516 CrossRef Medline
53. Begun, J., Lassen, K. G., Jijon, H. B., Baxt, L. A., Goel, G., Heath, R. J., Ng, A., Tam, J. M., Kuo, S. Y., Villablanca, E. J., Fagbami, L., Oosting, M., Kumar, V., Schenone, M., Carr, S. A., *et al.* (2015) Integrated genomics of Crohn's disease risk variant identifies a role for CLEC12A in antibacterial autophagy. *Cell Rep.* **11,** 1905–1918 CrossRef Medline
54. Ran, F. A., Hsu, P. D., Wright, J., Agarwala, V., Scott, D. A., and Zhang, F. (2013) Genome engineering using the CRISPR-Cas9 system. *Nat. Protoc.* **8,** 2281–2308 CrossRef Medline
55. Zhang, C., Tang, Y., Li, Y., Xie, L., Zhuang, W., Liu, J., and Gong, J. (2017) Unfolded protein response plays a critical role in heart damage after myocardial ischemia/reperfusion in rats. *PLoS One* **12,** e0179042 CrossRef Medline
56. Merrill, N. M., Schipper, J. L., Karnes, J. B., Kauffman, A. L., Martin, K. R., and MacKeigan, J. P. (2017) PI3K-C2α knockdown decreases autophagy and maturation of endocytic vesicles. *PLoS One* **12,** e0184909 CrossRef Medline
57. Mitsui, Y., Chang, I., Fukuhara, S., Hiraki, M., Arichi, N., Yasumoto, H., Hirata, H., Yamamura, S., Shahryari, V., Deng, G., Wong, D. K., Majid, S., Shiina, H., Dahiya, R., and Tanaka, Y. (2015) CYP1B1 promotes tumorigenesis via altered expression of CDC20 and DAPK1 genes in renal cell carcinoma. *BMC Cancer* **15,** 942 CrossRef Medline
58. Wang, Z., Bu, J., Yao, X., Liu, C., Shen, H., Li, X., Li, H., and Chen, G. (2017) Phosphorylation at S153 as a functional switch of phosphatidylethanolamine binding protein 1 in cerebral ischemia-reperfusion injury in rats. *Front. Mol. Neurosci.* **10,** 358 CrossRef Medline
59. van de Beek, M. C., Ofman, R., Dijkstra, I., Wijburg, F., Engelen, M., Wanders, R., and Kemp, S. (2017) Lipid-induced endoplasmic reticulum stress in X-linked adrenoleukodystrophy. *Biochim. Biophys. Acta* **1863,** 2255–2265 CrossRef Medline
60. Inoue, Y., Kawachi, S., Ohkubo, T., Nagasaka, M., Ito, S., Fukuura, K., Itoh, Y., Ohoka, N., Morishita, D., and Hayashi, H. (2017) The CDK inhibitor p21 is a novel target gene of ATF4 and contributes to cell survival under ER stress. *FEBS Lett.* **591,** 3682–3691 CrossRef Medline
61. Zhang, Q., Sun, J., Wang, Y., He, W., Wang, L., Zheng, Y., Wu, J., Zhang, Y., and Jiang, X. (2017) Antimycobacterial and anti-inflammatory mechanisms of baicalin via induced autophagy in macrophages infected with mycobacterium tuberculosis. *Front. Microbiol.* **8,** 2142 CrossRef Medline